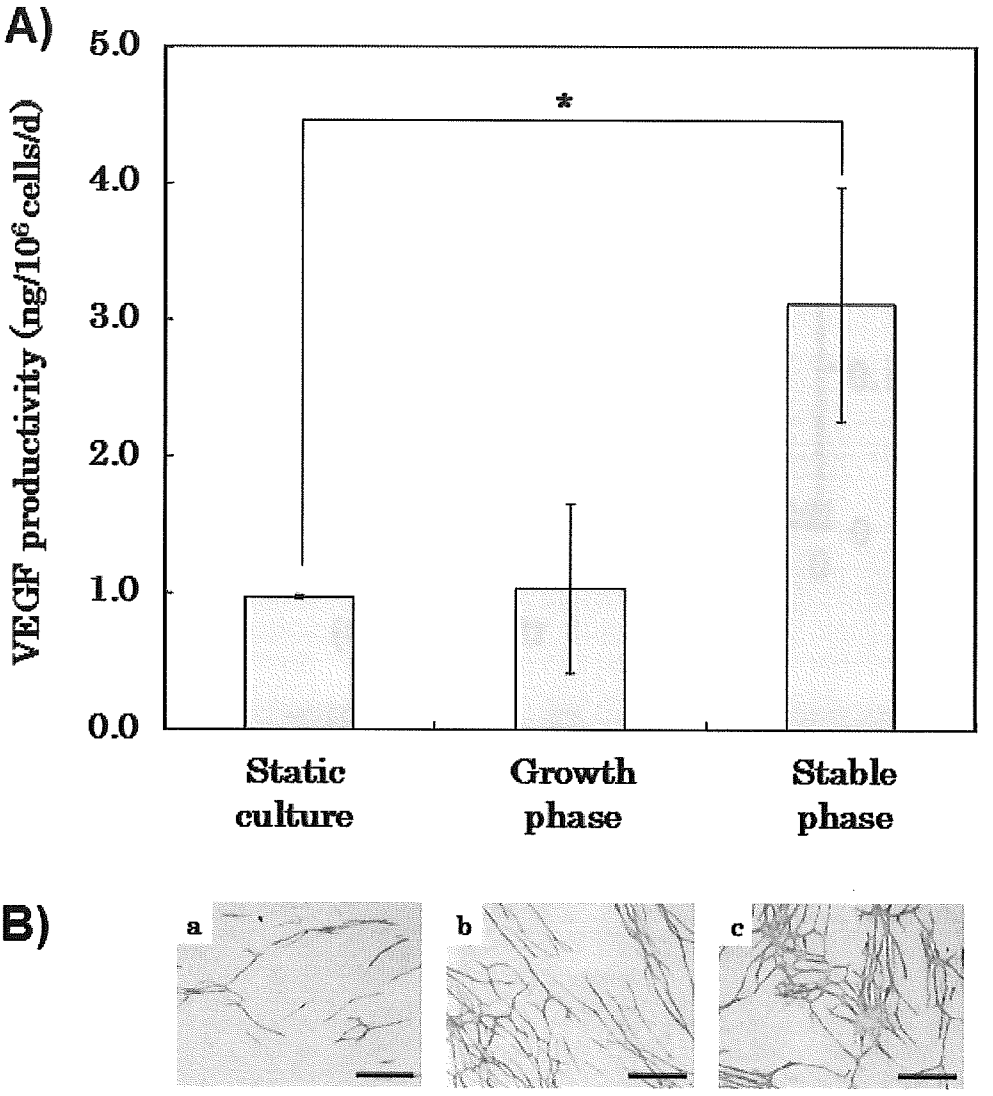

Fig. 3 **異なる増殖状態でのHepG2細胞のVEGF産生の差異**

通常の培養dishによる培養上清(static culture) 及びRFB培養の増殖期(growth phase)と定常期(stable phase)の培養上清を回収し、A) VEGFの産生量をELISA法により定量した。(* P <0.01) B) それぞれの培養上清を用いて血管新生アッセイを行った。a : static culture, b: growth phase, c : stable phase。

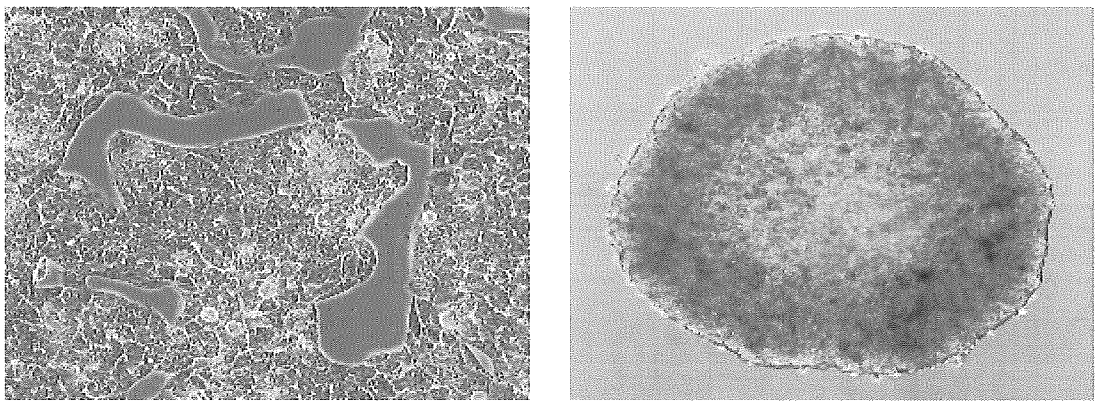

Fig. 4 **HepG2細胞のスフェロイド形成の様子**

HepG2細胞を通常の培養dish (plate)及びスミロン
セルタイト スフェロイド(spheroid)で培養した様子。

厚生労働科学研究費補助金（萌芽的先端医療技術推進研究事業）
分担研究報告

ヒト肝３次元培養系、マウス・ヒト肝細胞融合系による新規医薬品毒性評価系に関する基盤研究

遺伝子発現調節機構の解析に関する研究

分担研究者　　宮島　敦子　　国立医薬品食品衛生研究所薬理部　主任研究官

研究要旨：ヒト肝における種々の薬物動態関連遺伝子の発現を模倣する細胞系の構築を目指す上で、ヒト肝における種々の薬物動態関連遺伝子の mRNAレベルの解析は重要である。本研究では、ヒト肝における*CYP3A4*および関連薬物動態遺伝子の発現量の個体差について検討した。その結果、*CYP3A4*の発現量の個体差には、関連核内受容体遺伝子*PXR, CAR*の発現量の個体差が関与していることが示唆された。

A. 研究目的

医薬品および化学物質の有効性・安全性評価において、近年、実験動物を用いた試験法の限界が指摘され、ヒトにおける有効性・安全性を評価するための試験系の確立が必要になっている。ヒトの組織を用いた薬物代謝実験は、かつてミクロソームや S9 など肝細胞分画が用いられる事が多かったが、近年、ヒトの肝細胞を用いた試験系が、薬物動態を総合的に評価できることから有用視されてきている。しかしながら、現在利用できるヒトの肝細胞は、日本国内においては倫理的な問題、臓器移植法の問題があり、移植不適合臓器を研究に使用できず、海外からの輸入市販品に頼らざるを得ない。ヒトにおいて薬物の代謝に関わっている主要な薬物代謝酵素はチトクローム P450(CYP)であるが、CYP 活性量には、大きな個体差が存在することが知られている。インタクトな肝細胞を用いた試験系においても、各々の肝細胞が遺伝多型や薬歴（酵素阻害および誘導）などに由来する酵素活性の変動（個体差）を持つことを常に考慮しなければならない。そこで、インタクトな細胞の状態で CYP 活性を安定的に評価できる細胞の開発が望まれている。

本研究では、ヒト肝における種々の薬物動態関連遺伝子の発現を模倣する細胞系を目指しているが、そのためには、近年入手可能になったヒト肝組織において、薬物動態関連遺伝子のmRNAレベルの基礎データを取っておく必要があると考えられる。今年度は、ヒト肝組織における薬物動態遺伝子の発現量の個体差について検討した。特に、

薬物代謝において主要な役割を果たすCYP3A4には大きな個体差が存在することが知られているが、その個体差を説明し得る遺伝子多型は未だ報告されておらず多型以外の要因がむしろ積極的に関与していると考えられる。まず始めにヒト肝における、CYP3A4蛋白、*CYP3A4*遺伝子の発現量について検討し、さらに主要なCYP遺伝子の発現量および、関連受容体、転写因子遺伝子の発現量についても解析を進める。一方、本研究において、薬物代謝酵素遺伝子の発現調節機構の解析を進めるにあたり、インタクトなヒト肝細胞での研究は欠かす事ができない。そこで、本年度は予備実験として、現在市販されているヒト接着型凍結肝細胞の幾つかのロットについて比較検討し、細胞の回収、接着、生存率のスコアがよく薬物代謝酵素（*CYP1A1, 1A2*および*3A4*）の誘導が十分に観察できるものを選定した。

B. 研究方法

RNA画分の調製およびmRNA発現量の測定

ヒト肝臓組織は、獨協医科大学およびHS研究資源バンクより供給された転移性肝癌患者における肝臓非腫瘍部位24例を測定検体として使用した。検体は、male 15検体(0.625)， female 9検体(0.375)，average age±S.D.= 61.1±11.5であった。Total RNA画分の抽出は、RNAqueous Small Scale Phenol-Free Total RNA Isolation Kit (Ambion Inc., USA)により行った。Total RNAサンプルをoligo $d(T)_{16}$もしくはrandom primerによりRT反応を行い、cDNAを調製した。内在性コントロールとしてβ-actin (BACT)，GAPDH (glyceraldehyde-3-phosphate dehydrogenase)を用い、TaqMan probeを用いたreal-time PCR反応によりmRNA発現量を定量した。対象遺伝子として、薬物代謝酵素は、*CYP1A1, 1A2, 2B6, 2C8, 2C9, 2C18, 3A4, 3A5, 3A7, 3A43*を、核内受容体は *AHR, PXR, CAR, GR* および核内受容体お複合体を形成する*ARNT, RXRA*、転写因子は、*HNF1A* および *HNF4A*について測定した。内部標準物質として市販のヒトpoly (A)$^+$ RNA(Becton Dickinson, USA)サンプルを使用した。調製したRNA画分のqualityは、Agilent BioanalyzerによりrRNAの18S, 28Sのピークにより確認した。

Microsomal画分の調製および Western blot解析

ヒト肝臓組織をhomogenize後、遠心により（9,000×g, for 20 min at 4℃ and 105,000×g, for 60 min at 4℃)、 microsomal画分を調製した。蛋白定量は、BCA Protein Assay Kit(PIERCE, USA)により行った。CYP3A4, 3A5蛋白の検出は、WB-3A4 human CYP3A4 Western Blotting KitおよびWB-3A5 human CYP3A5 Western Blotting Kit (GENTEST, USA) を用いた。定量は市販のヒト発現系 microsome(baculovirus-mediated expression systems)(GENTEST,USA)により行った。

ヒト接着型凍結肝細胞における薬物代謝酵素誘導

ヒト接着型凍結肝細胞は、XenoTech(日本農産)、T-cubed(KAC)、In Vitro Technology (IVT)(チャールズリバー)より、各2ロットずつ購入した。(XenoTech: Lot 428,446、 T-cubed: Lot HH238, HH230、IVT: Lot NPV, LOF) 細胞は液体窒素冷却下で輸送および保存した。細胞（ー5 x10(6)cells /vial x2）の融解は、

Hepatocyte Isolation Kit (K2000) (XenoTech, USA)を用い添付の説明書に従って融解した。37℃温浴にて融解(1.5 min ±15sec)、percoll処理後、Lanford medium-10% FCSに懸濁した。トリパンブルー染色法により細胞数を計測し、生細胞数が$1x10^6$ cells/well(XenoTech)もしくは$0.75x10^6$ cells/well(T-cubed, IVT)となるように collagen-coated 12-well plateに播種した。培養4時間後に細胞をL-15 mediumで2回洗浄し、無血清のLanford mediumにて2日間培養した(24時間毎に培地交換)。次いで誘導培地(Lanford-0.1% DMSO,50uM Omeprazole (OME), or 25uM Rifampicin(RIF))に交換、24時間暴露し細胞を回収した。RNA画分は、RNeasy Mini Total RNA preparation kit (QIAGEN, USA)により調製した。薬物代謝酵素の誘導は、ヒト肝細胞のRNA画分と同様、TaqMan probeを用いたreal-time PCR反応によりmRNA発現量を定量した。対象遺伝子として、*CYP1A1, 1A2, 3A4, 3A5, PXR, CAR*について測定した。

(倫理面への配慮)

本研究に使用したヒト肝臓組織は、獨協医科大学およびHS研究資源バンクにおいて、正式なルートに基づいて書面にてドナーより同意を得て取得した試料である。また、本研究において購入したヒト凍結肝細胞はXenoTech、T-cubed、In Vitro Technology (IVT)において、正式なルートに基づいて書面にてドナーあるいはその近親者の同意を得て提供されたものである。いずれの試料も、ドナーを特定するような情報は一切消去され、個人を特定することは出来ないようにされており、提供者の人権を損害する危惧はない。提供された試料は本研究にのみ使用し、使用後は定められた基準に従い廃棄した。

C. 研究結果

ヒト肝における種々の薬物動態関連遺伝子の発現について

日本人24検体の肝組織を用いて、CYPおよび関連薬剤反応性遺伝子の発現量の個体差について検討した結果、*CYP1A1, 1A2, 2B6, 2C9, 3A4, 3A5, 3A43*のmRNA量の個体差は16-107倍、*AHR, PXR, CAR, GR*では5-40倍、CYP3A4, 3A5蛋白の個体差はそれぞれ9, 1560倍であった (Fig.1)。 microsome画分が調製できた23検体について、蛋白発現と遺伝子発現の相関について検討したところ、CYP3A4ではr=0.445, $p<0.05$, CYP3A5ではr=0.667, $p<0.01$の相関が観察された(Fig. 2)。 特に、CYP3A5の発現量は2相性を示した(Fig. 3)。

*CYP1A*遺伝子の発現については、*CYP1A1*と*1A2* のmRNA発現量は強く相関していたが、これら*CYP1A*と*AHR* mRNA発現量との相関は比較的弱かった(Fig.4)。*CYP2B, 2C, 3A*遺伝子の発現については、*CYP2B6, 2C9, 3A4* mRNA発現量は互いに相関し、*PXR, CAR*両受容体の発現量とも相関していた。一方、*GR* mRNAの発現量は今回測定したいずれの遺伝子のmRNA発現量とも相関がなかった。核内受容体と複合体を形成する*RXRA*の発現量は*PXR, CAR*と弱い相関が観察された。転写因子 *HNF4A* mRNAの発現量は、*CYP2B6, 2C9, CAR* mRNAの発現量と相関が観察された。また、*CYP3A4, HNF1A* mRNAの発現量とも弱い相関が観察された (Fig. 5) 。

ヒト接着型凍結肝細胞における薬物代謝酵素誘導について

購入した6ロットについて、各社より提供された、ドナー情報、細胞の生存率、代謝活性等についてまとめた（Table 1）。細胞融解percoll処理後のcell number、viability、recoveryについては、どのロットも高いviabilityが得られたが（92.4-96.9%）、生細胞数は TC 238, IV NPVではそれぞれ、2.90, 4.59x10^6 cellsと少なかった。IV LOFでは、培地交換時に剥がれて取り除かれる細胞が多かった。最終的なwell当りのRNA回収量は、0.77-5.38 ug/wellでばらつきが見られた。Xe 446, TC 238, IV NPVでRNAの回収量が多かった（Table 2）。*CYP1A1, 1A2*の誘導については、24時間のOME処理細胞により、*1A1*は30-131倍、*1A2*は21-233倍の誘導が観察された（Table 3）。この時の相対的なmRNA発現量について比較したところ、OME処理によって、*CYP1A1, 1A2*は同様に誘導されていた(Fig. 6)。また、DMSO処理サンプルによるbasalな*CYP1A2*発現量を比較したところ、Xe 446は他のロットに較べて発現量が低く、高い誘導倍率を示していた。一方、*CYP1A*の発現に関与する*AHR*の発現量については、DMSO, OME, RIF処理で差がなかった。次に、*CYP3A4*については、24時間のRIF処理により、13-140倍の誘導が観察された。相対的なmRNA発現量について比較したところ、TC 230は他のロットに較べてbasalな*3A4*発現量が高かった(Fig.7)。 RIFにより誘導発現したmRNAは、TC 238, TC 230が高かった。*CYP3A5*の発現量について比較したところ（測定はExon3/4 probeを使用）、TC 238の発現量は他のロットより高くOME, RIFによる誘導も観察されたが、他の5ロットでは、発現が低く、誘導もほとんど観察されなかった。*CYP3A4*の発現に関連する核内受容体*PXR, CAR*の発現については、6ロット間で大きな差はなく、24時間処理では、OME, RIFにより顕著な誘導は観察されなかった。

D. 考察

ヒト肝における種々の薬物動態関連遺伝子の発現について

日本人の肝組織24検体を用いて、薬物動態関連遺伝子の発現量の個体差について検討した結果、薬物代謝酵素*CYP1A1, 1A2, 2B6, 2C9, 3A4, 3A5, 3A43*のmRNA量の個体差は16-107倍であったのに対し、その発現制御に関わっていると考えられる核内受容体*AHR, PXR, CAR, GR*では個体差が5-40倍であり、下流の遺伝子の発現量の変動幅の方が大きかった。microsome画分が調製できた23検体について、蛋白発現と遺伝子発現の相関について検討したところ、*CYP3A4, 3A5*ともに相関が観察された。

特に、CYP3A5の発現量は2相性を示し、24検体のうち、3A5の発現量が低いものは11検体(0.478)で、日本人における3A5 *3/*3の頻度（0.74-0.77, 0.749）にほぼ対応していた。

*3 allele freq.= 0.74-0.77
(Hiratsuka et al. 2002, Fukuen et al. 2002),
*3 allele freq.= 0.759, *1/ *1 0.064, *1/ *3 0.353, *3/ *3 0.583 (n=187) Saeki et al. 2003)

*CYP1A*遺伝子の発現については、*CYP1A1*と*1A2* mRNA の発現量は強く相関していたが、*AHR* mRNA 発現量との相関は比較的弱かっ

た。また、*AHR*と複合体を形成する*ARNT*との相関は観察されなかった。これらの結果より、*CYP1A1, 1A2* mRNAの発現制御には、*AHR*が関与しているが、それ以外の因子も関与している可能性が示唆された。*CYP2B, 2C, 3A*遺伝子の発現については、測定した*CYP2B6, 2C9, 2C18, 3A4, 3A5, 3A7, 3A43*のうち、*CYP2B6, 2C9, 3A4* mRNA発現量は互いに相関し、*PXR, CAR*両受容体の発現量とも相関していた。核内受容体と複合体を形成するRXRAの発現量は、*PXR, CAR*と弱い相関が観察された。転写因子 *HNF4A* mRNAの発現量は、*CYP2B6, 2C9, CAR* mRNAの発現量と相関が観察された。また、*CYP3A4, HNF1A* mRNAの発現量とも弱い相関が観察された。以上より*CYP2B6, 2C9, 3A4* の発現量の個体差には、核内受容体*PXR, CAR*の発現量の個体差が関与していることが示唆された。

<u>ヒト接着型凍結肝細胞における薬物代謝酵素誘導について</u>

現在日本で購入できるヒト接着型凍結肝細胞は、XenoTech(日本農産)、T-cubed(KAC)、IVT(チャールズリバー、TMリサーチ)、Gentest(第一化学薬品)、RILD（チャールズリバー、第一化学薬品）の5社経由の細胞である。このうち倫理、在庫数、添付情報などを考慮してXenoTech、T-cubed、IVTの各2ロットについて検討することにした。この3社の供給する細胞情報は共通するものとして、ドナー情報（年齢、性別、人種、死因、アルコール、たばこ、drug歴、HCV, HBV,HIV,MCV陰陽性）、細胞情報（細胞数、生存率、接着率、薬物代謝酵活性（主なCYP, UGTほか））がある。XenoTech、IVTではこれらに加えてCYP1A2, 3A4の誘導結果、IVTではgenotype(*NAT, CYP2C19, 2D6, 2C9*)も添付されている。T-cubedの細胞に誘導データはないものの、日本に輸入されて後、KACにおいて実際に細胞を融解した際の細胞数、生存率、接着率情報が添付されていることに特徴がある。価格についても、XenoTechが～5 million/vial ¥11～12万円、T-cubedが～8 million/vial ¥8万円、IVTが～5 million/vial ¥13.8万円と様々であることから、細胞の回収、接着、生存率のスコアがよく、*CYP1A1, 1A2*および*3A4*の誘導が十分観察される良いロットを見つけて同じ細胞をまとめて購入した方がよいと考えた。実験は各社の推奨融解法、培養方法を比較検討し、共通のプロトコールにて（但しwellあたりの培養細胞数は実験結果により一部変更）行った。

購入した6ロットについての結果を、Cの研究結果に示したが、実際に融解してみると、percoll処理によりどのロットも高いviabilityが得られた。しかしながらrecoveryは29-97%で、ロットによりかなり異なっていた。最終的なwell当りのRNA回収量は、0.77-5.38 ug/wellでばらつきが見られたが、これは培地交換時に接着が不十分であった細胞は吸引されたためと考えられ、この値が最終的な細胞数を反映していると思われる。CYPの誘導については、添付のデータと誘導条件がそれぞれ異なるので一概に比較することはできないが、*CYP1A1, 1A2*で21-233倍、*3A4*で13-140倍であり、いずれのロットにおいても、*CYP1A1, 1A2, 3A4*ともに、十分な誘導が観察できた。もとのbasalのCYP1A1/2, 3A4の発現量が細胞により異なり、その値によって誘導倍率は異なってくるため、相対的な発現量も考慮する必要

がある。関連核内受容体の発現量を比較した結果、*AHR*発現量はOME処理により変化がなかった。これに対して、*PXR, CAR*の発現量はRIF処理により減る傾向が観察された。今回の検討では、細胞数の都合により誘導剤の処理時間を同じにするため、*CYP1A1/2, 3A4*両者の発現の誘導が観察できる24時間を選んだが、今後の研究においては、目的とする遺伝子の発現誘導時間に留意し、至適時間処理する必要があると思われる。*CYP3A5*の発現量について比較したところ（測定はExon3/4 probeを使用）、TC 238の発現量は他のロットより高くOME, RIFによる誘導も観察されたが、他の5ロットでは、発現が低く、誘導もほとんど観察されなかった。このことからTC 238は*3A5*1*を持つことが予想されるが、他の5ロットは*3A5*3/*3*である可能性が高い。CYP3A4遺伝子と3A5遺伝子は同じ染色体上の近隣に位置していることから、両者の発現を区別する上で、CYP3A5の発現量が高い細胞と低い細胞は有用であると思われる。細胞の回収、接着、生存率のスコア、*CYP1A1, 1A2*および*3A4*の誘導率、さらには細胞の価格も考慮し、2ロットを選定した。本年度の補正会計においてこれらの細胞をまとめて購入することができたので、今後の研究に利用する予定である。

E. 結論

本年度の研究により以下の点が明らかとなった。

1. ヒト肝における種々の薬物動態関連遺伝子の mRNAレベルの解析を行い主要な遺伝子の発現量のプロファイルを得た。
2. *CYP1A1, 1A2, 2B6, 2C9, 3A4, 3A5, 3A43*とその発現制御に関わっていると考えられる核内受容体*AHR, PXR, CAR, GR*の*発現量の個体差を比較した結果*、下流の遺伝子の発現量の変動幅の方が大きかった。
3. *CYP3A5*の発現量は2相性を示し、蛋白発現量とmRNA発現量は高い相関を示し、その頻度は、日本人における*3A5*3/*3*の頻度にほぼ対応していた。
4. *CYP3A4*遺伝子の発現量の個体差には、関連核内受容体*PXR, CAR*の発現量の個体差が関与していることが示唆された。

G. 研究発表

1. 論文発表

なし

2. 学会発表

Atsuko Miyajima-Tabata, Shogo Ozawa, Hiromasa Tanaka, Kenya Nakai, Momoko Sunouchi, Jun-ichi Sawada, Yuichiro Kamikawa, Keiichi Kubota, Hiroyasu Ogata, Yasuo Ohno The Crosstalk of Nuclear Receptors on the Expression of CYP Isoforms in Japanese Liver Tissue. ISSX/JSSX Meeting (Maui, Hawaii), Oct. 26, 2005

H. 知的財産権の出願・登録状況

なし

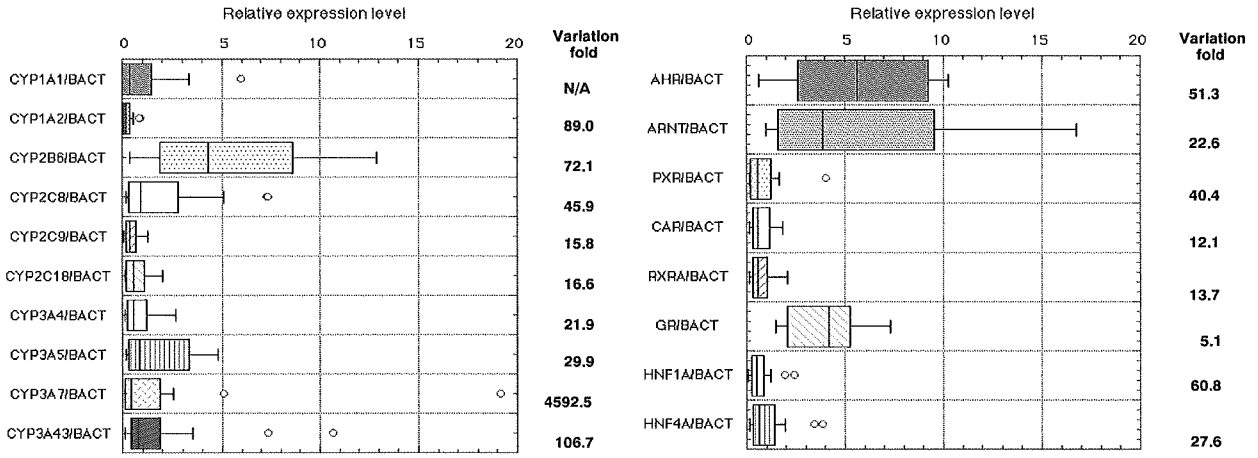

Fig. 1 Relative expression levels of *CYP* and its related nuclear receptor genes in liver tissues

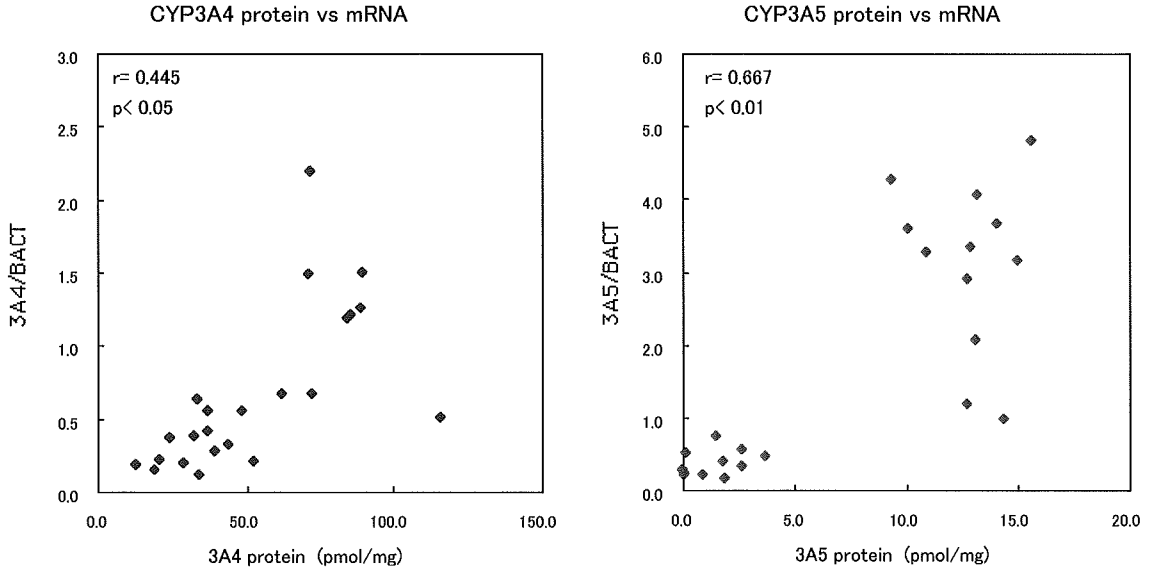

Fig. 2 Correlation between protein and mRNA expressions in CYP3A4, and 3A5

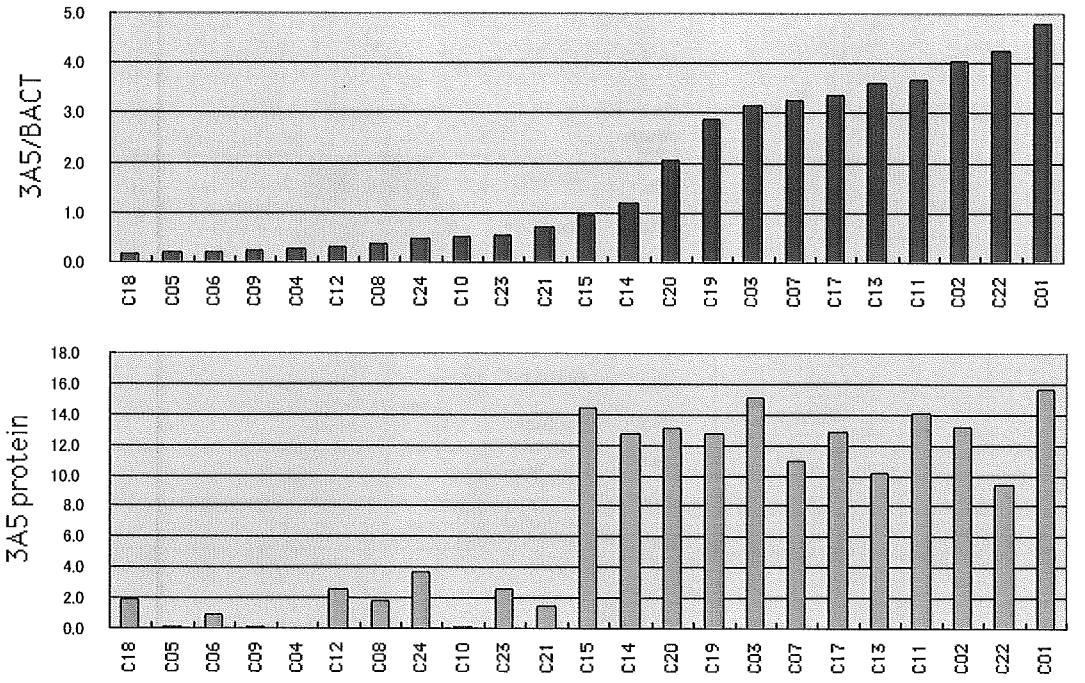

Fig. 3 Profiles of CYP3A5 mRNA and protein expressions

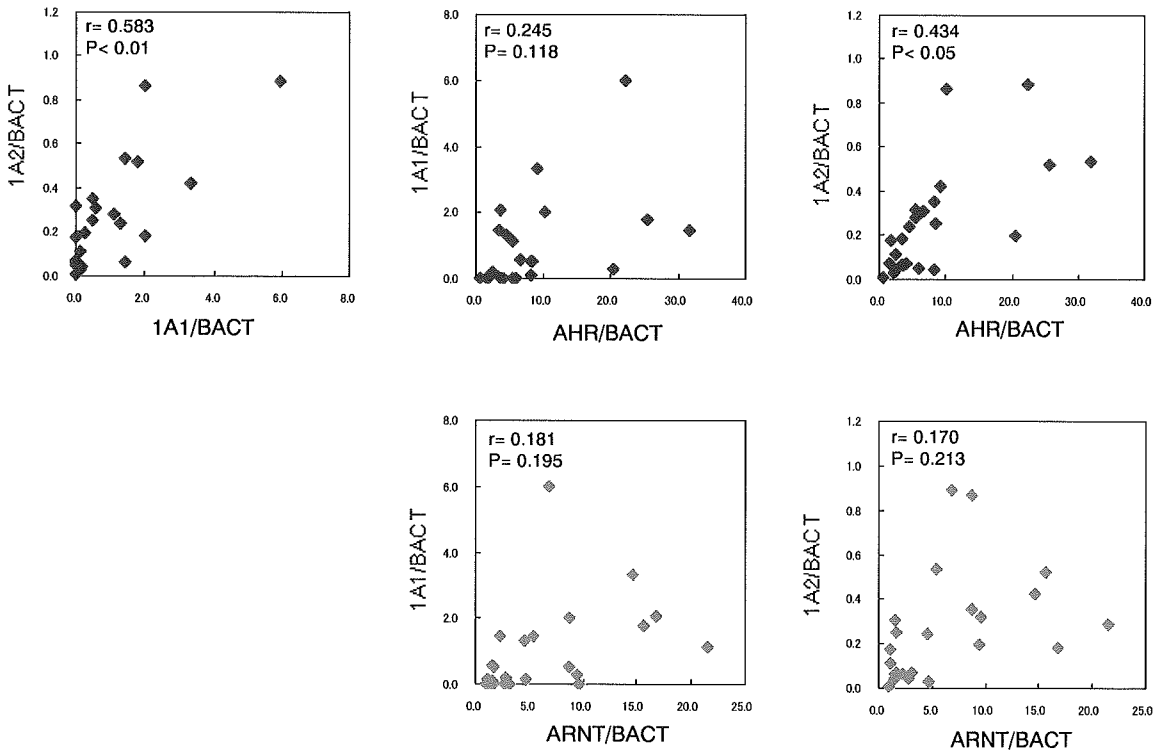

Fig. 4 Correlation of *CYP1As* mRNA levels with those of genes regulated commonly with *C YP1As*in liver tissues

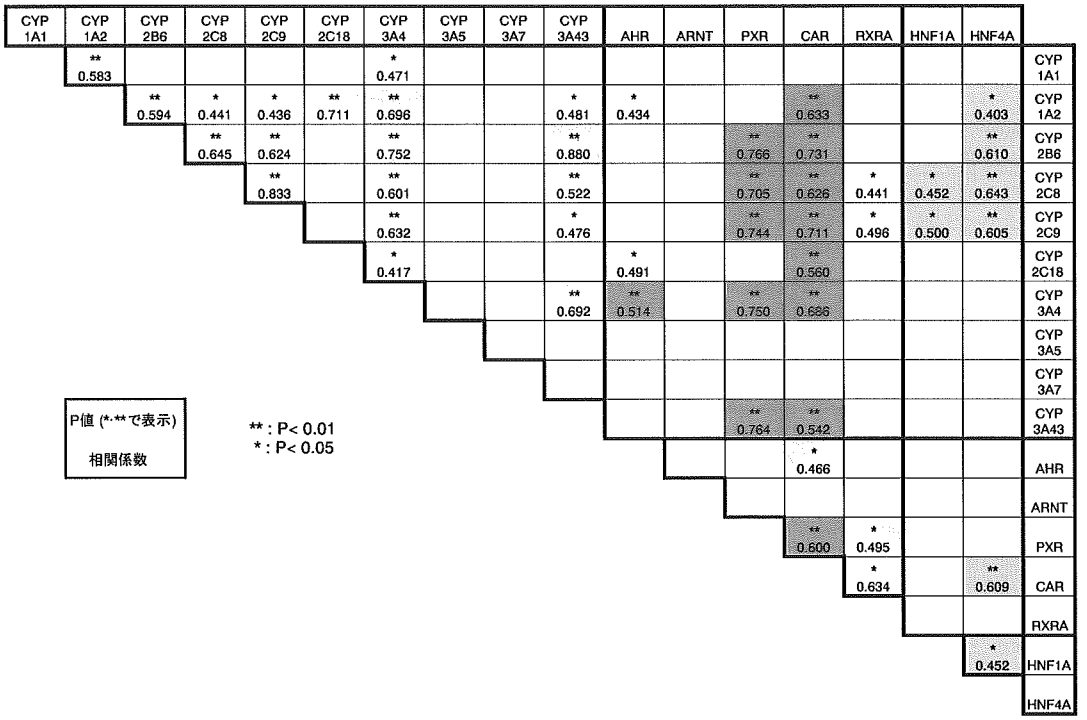

Fig. 5 Correlation of *CYP* mRNA levels with those of genes regulated commonly with *C YP*in liver tissues

XenoTech (日本農産)

Lot 428	gender	female	Lot 446	gender	male
	age/demographic	57/Caucasian		age/demographic	21/Caucasian
	cause of death	Head Trauma		cause of death	Head Trauma
	serology	CMV(+) HIV(-) HBV(-) HCV(-)		serology	CMV(-) HIV(-) HBV(-) HCV(-)
	yield (x10(6))/via	7.32		yield (x10(6))	7.80
	post thawing viab	93%			
	cell/vial	over 5 x 10(6) /1.5ml /vial		cell/vial	over 6 x 10(6) /1.5ml /vial
		¥110,000/vial			¥125,000/vial
data	3A4/5 Test 6b	234 pmol/10(6)cells/min	data	3A4/5 Test 6b	223 pmol/10(6)cells/min
	Induction 1A2	21.5 fold (33uM b-NF, mRNA/GAPDH)		Induction 1A2	53.5 fold (100uM Ome, Phenacetin o-deethy)
	Induction 3A4	73.8 fold (20uM Rif, mRNA/GAPDH)		Induction 3A4	12.8 fold (10uM Rif, Midazolam 1'-hydoxy)

T-cubed (KAC)

HH238	gender	female	HH230	gender	female
	age/demographic	10/Caucasian		age/demographic	47/Caucasian
	cause of death	Head Truma		cause of death	CVA (past medical histry, smoke N, alcohol Y, drug N)
	serology	HIV(-) HBV(-) HCV(-) RPR(-) HTLV(-)		serology	HIV(-) HBV(-) HCV(-) RPR(-) HTLV(-)
	yield (x10(6))/via	9.8 (KAC 4.36)		yield (x10(6))/via	10.9 (KAC 9.8)
	post thawing viab	84% (KAC 67.8%)		post thawing viab	88.8% (KAC 81.25%)
	plating efficiency	60% (KAC 80%)		plating efficiency	80% (KAC 70%)
	cell/vial	over 8 x 10(6) /1.5ml /vial		cell/vial	over 8 x 10(6) /1.9ml /vial
		¥80,000/vial			¥80,000/vial
data	3A4/5 Test 6b	17.75 pmol/10(6)cells/min	data	3A4/5 Test 6b	108.3 pmol/10(6)cells/min
	UDP-GT, FMO,ST,GST			UDP-GT, FMO,ST,GST	
	induction data	no		induction data	

IVT (チャールズリバー)

Lot NPV	gender	Female	Lot LOF	gender	Female
	age/demographic	40/Caucasian		age/demographic	54/Caucasian
	cause of death	Accidental overdose		cause of death	Cardiac Arrest
	serology	CMV(+) HIV(-) HBV(-) HCV(-)		serology	CMV(-) HIV(-) HBV(-) HCV(-)
		Tabacco Y, Alcohol N, Substance Y			Tabacco Y, Alcohol N, SubstanceN
	yield (x10(6))/via	5.0		yield (x10(6))	5.0
	post thawing viab	75%		post thawing viab	86%
	cell/vial	5 x 10(6) /1ml /vial		cell/vial	5x 10(6) /1ml /vial
		¥138,000/vial			¥138,000/vial
data	3A4/5 Test 6b	43 pmol/10(6)cells/min	data	3A4/5 Test 6b	102 pmol/10(6)cells/min
	Induction 1A2	12.0 fold (50uM OME 48h, activity)		Induction 1A2	14.7 fold (50uM OME 48h, activity)
	Induction 3A4	6.13 fold (25uM RIF 48h, activity)		Induction 3A4	5.80 fold (25uM RIF 48h, activity)
	genotype	NAT1,2, 2C19,9,2D6		genotype	NAT1,2, 2C19,9,2D6

Table 1 Informed data of cryopreserved hepatocytes

	infromed data		cell purification with Percoll methods			
	x10(6)cells/ vial	viability (%)	total x10(6)cells	viability (%)	recovery (%)	inoculate well no
Xe 428	7.32	93	11.77	96.6	80.4	11 (1x10(6))
Xe 446	7.80		8.83	96.3	56.6	8 (1x10(6))
TC 238	9.80 (KAC 4.36)	84 (KAC 67.8)	4.59	96.4	23.4(52.6)	6 (0.75x10(6))
TC 230	10.9 (KAC 9.80)	88.8 (KAC 81.25)	8.09	96.9	37.1(41.3)	10 (0.75x10(6))
IV NPV	5.0	75	2.90	92.4	29.0	3 (0.75x10(6))
IV LOF	5.0	86	9.73	94.5	97.3	12 (0.75x10(6))

	4h	final (72 h incubation)		
	plating efficiency(%)	x 10(6)cells /wells	recovery (%)	Ave.of RNA (ug/well)
Xe 428	69.8	0.42	42	2.23
Xe 446	83.8	0.39	39.1	4.90
TC 238	74.2	–	–	5.38
TC 230	82.3	0.18	23.9	1.73
IV NPV	81.9	–	–	4.29
IV LOF	87.3	0.3	40.2	0.77

Table 2 Cell recovery and viability of cryopreserved hepatocytes

	Fold induction (mRNA expression/GAPDH)					
	CYP1A1 (24h)	CYP1A1 (48h)	CYP1A2 (24h)	CYP1A1 (48h)	CYP3A4 (24h)	CYP3A4 (48h)
Xe 428	48.1	14.9 (n=1)	23.1	13.0 (n=1)	14.2	42.5 (n=1)
Xe 446	130.9	—	232.9	—	16.0	—
TC 238	57.1	—	633	—	138.8	—
TC 230	30.3	—	17.1	—	13.3	14.4 (n=1)
IV NPV	32.5 (n=1)	—	31.4 (n=1)	—	19.1 (n=1)	—
IV LOF	29.9	—	20.8	—	14.9	13.5

Table 3 CYP induction on platable cryopreserved hepatocytes

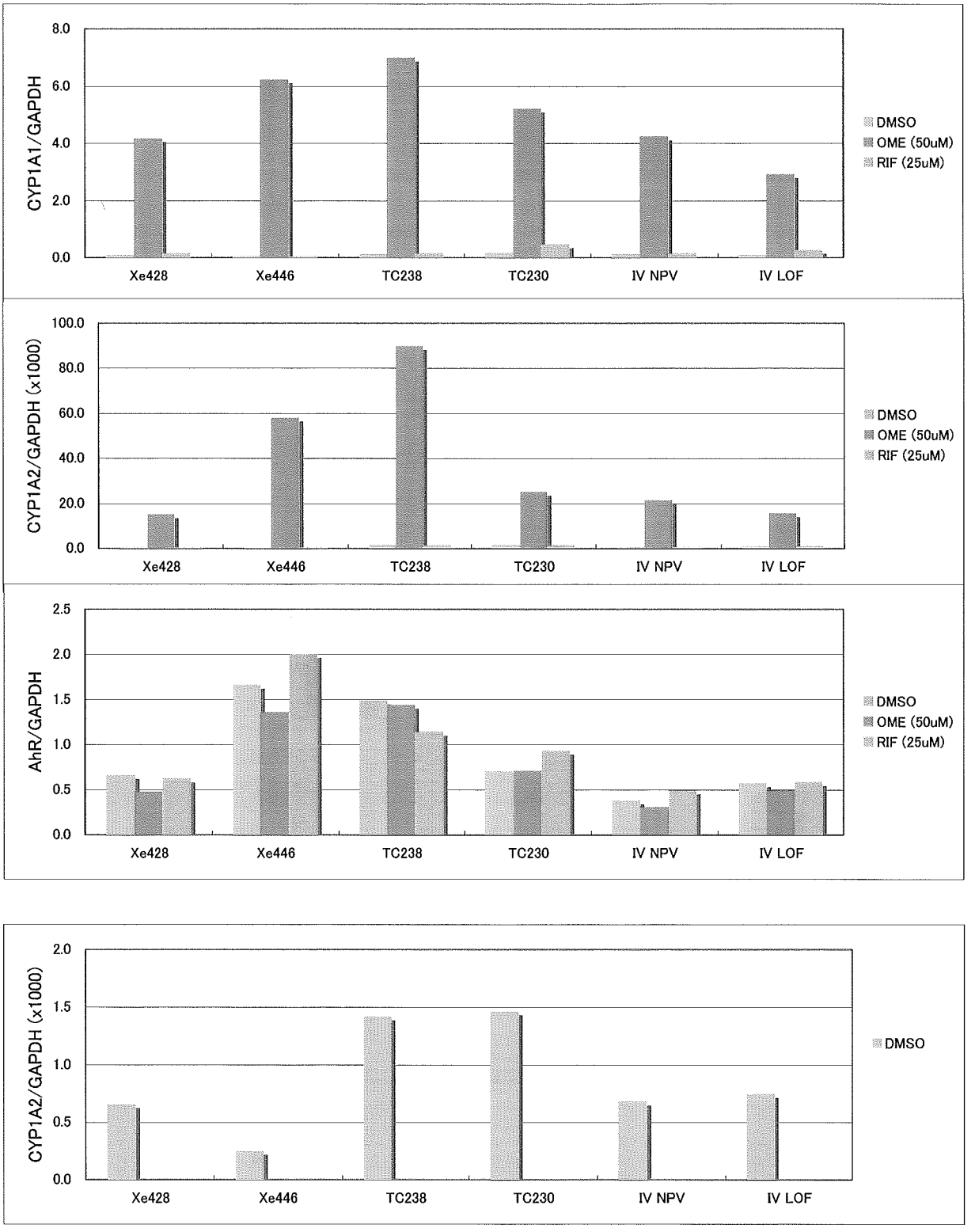

Fig. 6 Relative expression levels of CYP1As and related receptor genes

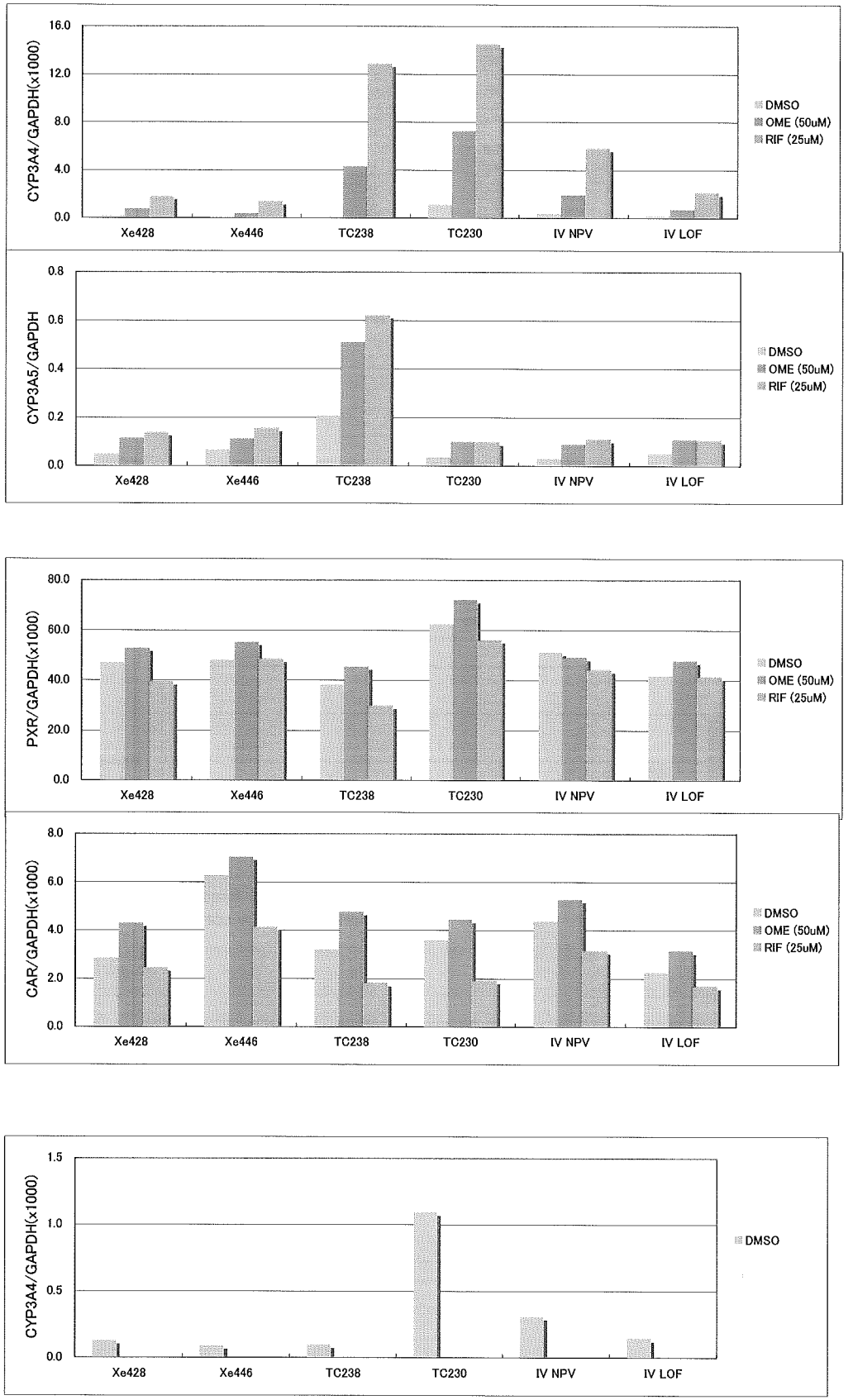

Fig. 7 Relative expression levels of CYP3As and related receptor genes

研究成果の刊行に関する一覧表レイアウト

書籍

著者氏名	論文タイトル名	書籍全体の編集者名	書　籍　名	出版社名	出版地	出版年	ページ

雑誌

発表者氏名	論文タイトル名	発表誌名	巻号	ページ	出版年
Tomokatsu Hongo, Mariko Kajikawa, Seiichi Ishida, Shogo Ozawa, Yasuo Ohno, Jun-ichi Sawada, Yoichi Ishikawa, Hiroyuki Honda	Gene expression Property of High-density three-dimensional tissue of HepG2 cells formed in radial-flow bioreactor	Journal of Bioscience and Bioengineering	101	111-999	2006

JOURNAL OF BIOSCIENCE AND BIOENGINEERING
Vol. 101, No. 3, 111–999. 2006
DOI: 10.1263/jbb.101.000

Gene Expression Property of High-Density Three-Dimensional Tissue of HepG2 Cells Formed in Radial-Flow Bioreactor

Tomokatsu Hongo,[1,4] Mariko Kajikawa,[1] Seiichi Ishida,[2] Shogo Ozawa,[2] Yasuo Ohno,[2] Jun-ichi Sawada,[3] Yoichi Ishikawa,[1] and Hiroyuki Honda[4]*

ABLE Corporation, 4-15 Higashigoken-cho, Shinjyuku-ku, Tokyo 162-0813, Japan,[1] Division of Pharmacology, National Institute of Health Sciences, 1-18-1 Kamiyoga, Setagaya-ku, Tokyo 158-8501, Japan,[2] Division of Biochemistry and Immunochemistry, National Institute of Health Sciences, 1-18-1 Kamiyoga, Setagaya-ku, Tokyo 158-8501, Japan,[3] and Department of Biotechnology, School of Engineering, Nagoya University, Furo-cho, Chikusa-ku, Nagoya, Aichi 464-8603, Japan[4]

Received 3 October 2005/Accepted 20 December 2005

In our previous study, we examined three-dimensional culture using 5-ml radial-flow bioreactor (RFB) and showed that genes encoding cell cycle related proteins were suppressed in a stable phase. In this study, we analyzed the gene expression profiles of RFB-cultivated HepG2 cells and found that vascular endothelial growth factor (VEGF) production was strongly induced in the stable phase compared with the growth phase or static two-dimensional culture. When human umbilical vein endothelial cells (HUVECs) were grown under the conditioned medium of the stable phase, it was found that the formation of new blood vessels was induced in the angiogenesis model. DNA microarray analysis showed that the expression levels of both genes related to cell cycle arrest and which are known as tumor markers have increased in the stable phase. This result suggests that HepG2 cells in the stable phase maintain an active tumor phenotype. In addition, the expression of genes induced in the hypoxic condition was also induced in the stable phase. When the culture was carried out under a higher dissolved oxygen (DO) concentration, VEGF production did not decrease significantly and the new blood-vessel-forming ability of the conditioned medium was not suppressed. This suggests that the induction of VEGF production in a stable phase is not affected by DO during the tested level. These results suggest that the RFB cell culture system may be used to assess tumor progression mechanism under three-dimensional condition *in vitro*.

[Key words: three-dimensional high-density cell culture, radial-flow bioreactor, DNA microarray]

Recently, many types of bioreactors for three-dimensional high-density cell culture have been developed since these bioreactors contribute to the construction of highly functional tissue-like structures. The cellular functions of the constructed structure were measured and compared with those of two-dimensional static culture and it has been reported that some cell functions were improved (1–6). However, whole gene profiles under three-dimensional high-density culture remain unclear and genetic evidence of the effectiveness of three-dimensional high-density culture remains unclarified. Although Vladimir *et al.* (7) showed the difference between static culture and three-dimensional culture using the rotary cell culture system, there was not any explicit feature on their listed genes.

In our previous study (8), we demonstrated that the hepatoblastoma cell line, HepG2, can be cultured in a radial-flow bioreactor (RFB) for more than two weeks. The glucose consumption was almost stable after day 10 and the time-lapse changes in lactic acid production, glutamine consumption, and ammonia production were almost the same as that of glucose. From the preliminary experiment using DNA microarray, it was found that the expressions of genes related to cell cycle were suppressed and cells remained in the G0/G1 phase at the stable phase. The diameter of aggregated cells in the RFB was more than 200 μm and maintained albumin production. This is important information regarding cancer progression. From their clinical experience handling cancer patients, Aguirre *et al.* (9) showed that some primary cancers and most metastatic lesions undergo a period of dormancy before progressive growth. For progressive growth, tumor angiogenesis must be induced (10). Tumor dormancy is defined as a state of angiogenic independent growth in which solid tumor growth does not often exceed 2 mm in diameter (11). In addition, tumor cells during tumor dormancy generally remain in the G0/G1 phase. Some induction mechanisms of G0/G1 arrest have been clarified. Aguirre *et al.* (9) showed that the decrease in the urokinase plasminogen activator receptor level in human carcinoma HEp3 cells induced a protracted state of tumor dormancy with G0/G1 arrest. This recent study revealed that oncogene inactivation in liver cancer resulted in the rapid loss of the

* Corresponding author. e-mail: honda@nubio.nagoya-u.ac.jp
phone: +81-(0)52-789-3215 fax: +81-(0)52-789-3214

expression of the tumor marker protein, alpha-fetoprotein (AFP), the increase in the expression of liver cell markers, cytokeratin 8 and carcinoembryonic antigen, and the induction of tumor dormancy (12). Considering these results, tumor dormancy may be defined as (i) three-dimensional cancer cell aggregation without neovascularization, (ii) G0/G1 arrest under a dormant condition, (iii) the induction of angiogenesis and (iv) the downregulation of some tumor marker proteins in a dormant condition. Among these definitions, we assumed that the first and second definitions were reflected in our previous study (8). Therefore, we hypothesized that the HepG2 cell growth in the RFB is similar to cancer growth in patients; hence, we used the RFB culture system as *in vitro* model of cancer progression.

To demonstrate our hypothesis, we first investigate in the present paper the difference in the gene expression level between the growth phase and the stable phase during the RFB cultivation of HepG2 cells. We show also identified genes with induced expression, such as insulin-like growth factor binding protein 3 (IGFBP-3) and vascular endothelial growth factor (VEGF). IGFBP-3 is a mediator of the growth suppressing signals of cells (13). Hence, VEGF is one of the most potent and specific angiogenic factors of tumor-induced angiogenesis (14, 15). The clinical importance of VEGF for tumor growth is supported by the fact that most tumors produce VEGF and the inhibition of VEGF-induced angiogenesis significantly inhibits tumor growth *in vivo* (16–18).

Next, we demonstrate that the conditioned medium of the stable phase during the RFB cultivation of HepG2 cells induced both the proliferation of human umbilical vein endothelial cells (HUVECs) and angiogenesis *in vitro*. Under a higher dissolved oxygen (DO) concentration during the RFB cultivation of HepG2 cells, the productivity of VEGF at the stable phase is suppressed incompletely. Compared with static culture condition, three-dimensional high-density culture in the RFB mimics normal physiological condition and our results indicate that the RFB culture of cancer cells will contribute greatly in clarifying the mechanism of the tumor growth progression *in vitro*.

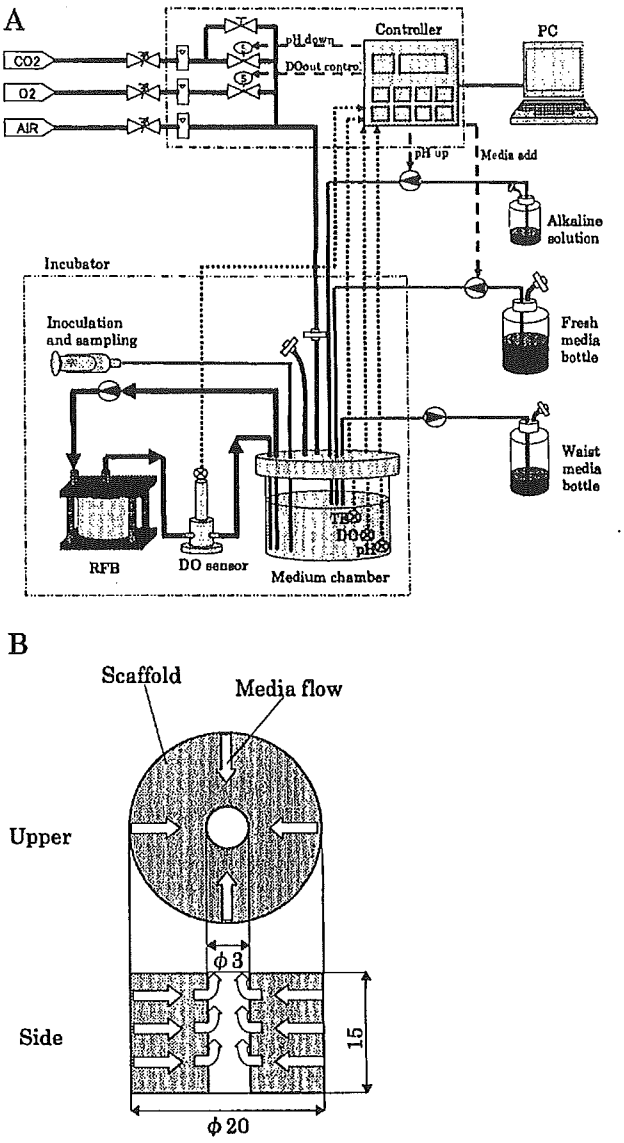

FIG. 1. Schematic of RFB cell culture system. (A) Culture system flow, (B) inner space of 5-ml RFB.

MATERIALS AND METHODS

Culture of HepG2 cells Hepatoblastoma cell line, HepG2, was obtained from American Type Culture Collection (Rockville, MD, USA). HepG2 cells were cultured in tissue culture dishes (59 cm^2; BD Biosciences, San Jose, CA, USA) and cell passaging was performed as described previously (8). Conditioned medium from static culture was collected from the culture dishes and stored at −80°C.

Culture of HUVECs Human umbilical vein endothelial cells (HUVECs) were obtained from Takara Bio (Kyoto). HUVECs (1×10^5 cells) were cultured in tissue culture flask (25 cm^2; BD Biosciences) with 5 ml of EBM-2 (Takara Bio) at 37°C in an incubator containing 5% CO_2. Cell passasing was performed every 3 d with trypsin/EDTA (0.05% trypsin, 0.53 mM EDTA-4Na; Gibco/BRL, Gaithersburg, MD, USA), which was utilized to detach the cells.

Culture in RFB A 5 ml RFB (ABLE, Tokyo) and an RFB cell culture system shown in Fig. 1 were used in this study for the culture of HepG2 cells as described previously (8). Hydroxyl apatite (Pentax Corporation, Tokyo) with a diameter of 0.6–1.0 mm was used as a scaffold. The relatively large particle contributes in reducing the back pressure of the fixed bed and provides much space for cell growth. The particles were filled in the inner space of the RFB (Fig. 1B). Homogeneous flow was observed from a tracer experiment using dye. HepG2 cells at 3×10^7 were inoculated into the chamber medium and circulated between the chamber medium and the RFB at 7 ml/min. After 16 h from inoculation, there were no remaining cells in the chamber medium. The volume of the chamber medium was maintained at 200 ml and fresh medium was added continuously from the third day. The flow rate of the fresh medium was 250 ml/d. The DO concentration of the effluent of the RFB was controlled at 4.0 ppm. Under a higher DO concentration, the effluent DO concentration was controlled at 8.0 ppm. pH was controlled at 7.6 and the measured concentrations of glucose, lactic acid, glutamine and ammonia in the culture media were controlled by BF-4 (Oji Scientific Instrument, Amagasaki). The cell counts in the RFB were determined on the basis of glu-

cose consumption rate. Conditioned medium was collected from the chamber medium at 7 d (growth phase) and 17 d (stable phase) and stored at −80°C. VEGF concentration in the medium was measured using the 96-wells-VEGF Human Assay kit (Amersham Biosciences UK limited, Buckinghamshire, UK).

mRNA isolation and DNA microarray analysis After culturing the HepG2 cells for 7 and 17 d in the RFB, mRNA was isolated from the scaffold as described previously paper (8). Samples were collected from three points in the RFB (peripheral, middle and central points). The conversion of total RNA (10 μg) to the target for Affymetrix GeneChip DNA microarray (Affymetrix, Santa Clara, CA, USA) hybridization was performed according to the manufacture's instruction. DNA microarrays were scanned and obtained images were analyzed using the GeneChip Expression Analysis Software (ver. 5.0) (Affymetrix). DNA microarray analysis was performed in duplicate for each sample and the average signal intensities of 7 d and 17 d were calculated. The induced genes in the stable phase were identified on the basis of the following scheme described below: (i) genes whose expression levels on 17 d when divided by the data on 7 d yielded a value higher than 3, (ii) genes whose expression levels from a duplicate analysis were within 1.5-fold margin of increase, (iii) genes whose p-value was less than 0.01 when the t-test was performed on the microarray data from 7 d to 17 d. RFB culture was carried out twice for 7 d and 17 d. The four kind of list of induced genes were compared and genes that were listed in all four kinds of list were selected.

HUVEC proliferation assay HUVECs (1×10^5 cells) were inoculated in tissue culture flask (25 cm^2) containing 5 ml of EBM-2 and cultured for 24 h. After EBM-2 was removed, HUVECs were treated with 5 ml of the collected conditioned medium from the RFB culture for 48 h. Dulbecco's modified Eagle medium (DMEM; Gibco/BRL) was used for treating the negative control and EBM-2 was used for treating the positive control. After the cultivation under each condition, HUVECs were collected from the culture flasks and the number of cells was counted using a hemocytometer. The cell numbers of the HUVEC culture treated with the conditioned medium from the RFB culture or of the negative control were divided by the cell number of the positive control and the resulting ratio was defined as ratio to positive control. The VEGF concentration of the conditioned medium was measured as described above and the experiments were performed under the same levels of VEGF concentration.

Blood vessel formation assay Blood vessel formation assay was performed using an angiogenesis kit (Kurabo Industries, Osaka). Conditioned medium was diluted with the control medium supplied in the kit at 1:1. Diluted medium was added to the corresponding well and incubated according to the manufacturer's instruction. VEGF-A (Kurabo) was added to the control medium (final concentration: 10 ng/ml) and this medium was used as control. Newly formed blood vessels were stained by using the tubule staining kit (Kurabo) and observed by light microscopy. The length of blood vessels was analyzed by angiogenesis image analyzer (Kurabo). Angiogenesis ratio to control with 10 ng/ml was calculated by divided by the pixel obtained from control.

RESULTS

DNA mircoarray analysis To clarify further the cell functions of HepG2 cells cultured in the RFB, we performed DNA microarray analysis with respect to cell samples from three points in the RFB. There were no significant differences between the three points (data not shown); thus the mean gene expression level from the three points was calculated and utilized in the analysis. Since HepG2 cells continuously grow forming multilayers even though the culture was already confluent, making it hard to achieve a stable growth condition of HepG2 2D culture because of confluency, we did not compare the gene expression profile of subconfluent HepG2 2D culture with that of confluent HepG2 2D culture. Then, the gene expression analysis of the stable phase was compared with that of the growth phase in 3D culture. As a result, 18 genes were selected as the genes induced in the stable phase. These selected genes are listed in Table 1. Okino *et al.* (19) reported that the expression of growth factor receptor-bound protein 10 (Grb10) mRNA in transformed primary cervical squamous cells was upregulated compared with noncancerous uterine squamous cells. Suganuma *et al.* (20) reported that angiotensin II receptor, type 1 (AT1R) was expressed in invasive ovarian adenocarcinomas. Except for these genes, six genes whose expression is common in cancer tissue exist (21–25). In addition, VEGF listed in Table 1 is known as a mitogen that specifically acts on endothelial cells and a major regulator for the induction of angiogenesis in tumors (14, 15).

On the other hand, insulin-like growth factor binding pro-

TABLE 1. Genes whose expressions were induced during stable phase

Gene	Accession no.	Fold
Insulin-like growth factor binding protein 3	BF340228	11.09
Growth factor receptor-bound protein 10	U66065	5.11
Angiotensin II receptor, type 1	NM_000685	4.65
B cell RAG associated protein	NM_014863	3.97
Apolipoprotein L, 1	AF323540	3.89
A kinase (PRKA) anchor protein (gravin) 12	AB003476	3.83
Sortilin-related receptor, L(DLR class) A repeats- containing	AV728268	3.64
Vascular endothelial growth factor	AF022375	3.43
Basic helix- loop- helix domain containing, class B, 2	BG326045	3.41
Adrenomedullin	NM_001124	3.34
Family with sequence similarity 13, member A1	NM_014883	3.34
Solute carrier family 2 (facilitated glucose transporter), member 3	NM_006931	3.32
KIAA1199 protein	AB033025	3.28
Lysyl oxidase	NM_002317	3.27
Ribonuclease T2	NM_003730	3.15
Mitochondrial ribosomal protein S6	AI867198	3.14
Carbonic anhydrase IX	NM_001216	3.10
Solute carrier organic anion transporter family, member 4A1	NM_006342	3.00

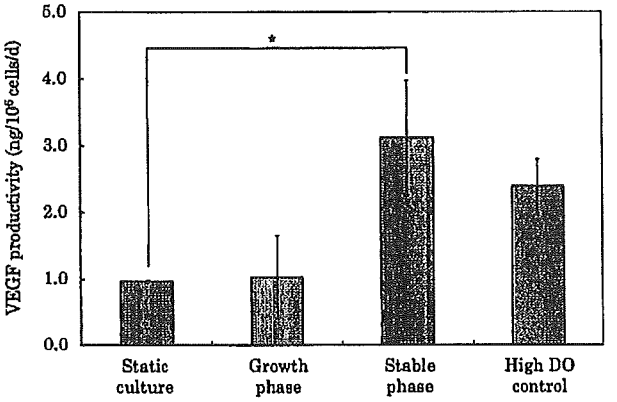

FIG. 2. VEGF productivity of HepG2 cells under static and 3D cultures in RFB. Static culture, culture in static culture flask; growth phase, culture in 5-ml RFB for 7 d; stable phase, culture 5-ml RFB for 17 d; high DO control, culture 5-ml RFB for 17 d below 8.0 ppm concentration. Asterisks indicate a significant difference between the static culture and stable phase (* $P<0.01$). Values are expressed as mean±SD for two independent cultures.

tein 3 (IGFBP-3) was also listed in Table 1. Treatment of hepatocellular carcinoma with IGFBP-3 led to a significant reduction in cell proliferation (26). In addition, A kinase anchor protein 12 and lysyl oxidase are known as tumor suppressor genes (27). In our previous report, cell cycle in the RFB cell culture system at the stable phase was arrested in most cells (8). Therefore, these results suggest that the stable phase of the RFB cultivation of HepG2 cells mimics the dormancy phase of tumor progression.

Production of VEGF during RFB cultivation

Whereas the above complex patterns of gene expression were demonstrated, there was a marked induction of VEGF expression which serves an important function in highly proliferating tumors. To demonstrate that HepG2 cells cultured in the RFB can release VEGF into the culture medium, we measured VEGF concentration and VEGF productivity was calculated. Figure 2 shows the VEGF productivity during the static culture, exponential growth phase and stable growth phase of the cell culture. VEGF productivity during the growth phase was almost the same as that during the static phase. However, VEGF productivity during the stable phase was approximately threefold higher than that of the static culture. The mean VEGF concentrations in the culture media were 51.5 pg/ml during the stable phase and 20.5 pg/ml during the growth phase. The calculated VEGF production rates were 1700 mg/d during the stable phase and 700 mg/d during the growth phase. Cell number was calculated on the basis of glucose consumption and the glucose consumption rates were 3.5×10^{-3} mol/d during the stable phase and 2.9×10^{-3} mol/d during the growth phase. Moreover, since the RFB culture was carried out by fed-batch operation, glucose (1.6–2.0 g/l) and glutamine concentrations in the culture media were not decreased and lactic acid and ammonia in the culture media were not excessively accumulated. Sone *et al.* (28) reported that VEGF production rate in bovine retinal pigmented epithelial cell culture was significantly increased by a decrease in glucose concentration from 5.5 to 0.5 mM, but not by a decrease in glucose

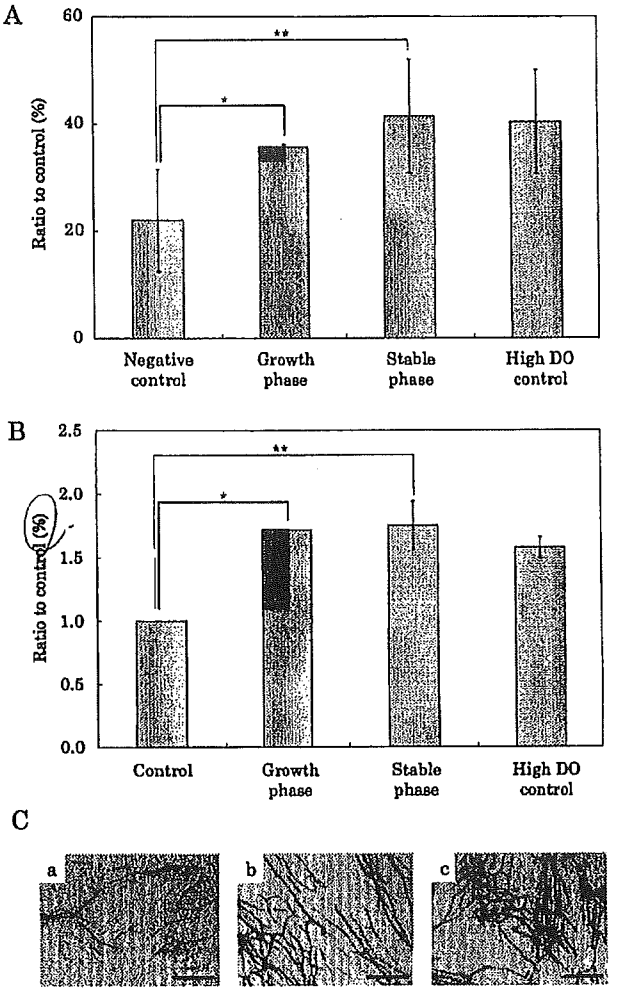

FIG. 3. Effects of conditioned medium on cultured HepG2 cells in 5-ml RFB. (A) HUVEC proliferation rate. The VEGF concentrations are 0 ng/ml (negative control), 4.8 ng/ml (growth phase), 4.6 ng/ml (stable phase), and 4.3 ng/ml (high DO control). The number of HUVECs cultured with the conditioned medium or in the negative control was divided by the number of cells in the positive control and the calculated ratio was defined as ratio to positive control. Asterisks indicate a significant difference (* $P<0.01$, ** $P<0.01$). Values are expressed as mean±SD for four independent cultures. (B) Angiogenesis assay. The VEGF concentrations are 10 ng/ml (control), 4.8 ng/ml (growth phase), 4.6 ng/ml (stable phase), and 4.3 ng/ml (high DO control). Ratio to control was calculated by divided by the pixel obtained from control. Asterisks indicate a significant difference (* $P<0.01$, ** $P<0.05$). Values are expressed as mean±SD for four independent cultures. (C) Light microscopic observations of newly formed blood vessels. a, Control; b, growth phase conditioned medium; c, stable phase conditioned medium. The bars represent 100 μm.

concentration from 16.5 to 5.5 mM. Therefore, we considered that the difference in VEGF productivity is not due to changes in the nutrient concentration in the culture media.

Next, HUVEC proliferation induced by the released VEGF in the conditioned medium of the RFB was also investigated. As shown in Fig. 3A, HUVEC proliferation was induced by the addition of the conditioned medium. When the same concentration of VEGF was used, the same proliferation rate was observed during the growth phase and the sta-

ble phase. Angiogenesis assay was also performed using the conditioned medium of the RFB. As shown in Figs. 3B and 3C, angiogenesis was observed and the ratio of blood vessel formation was almost the same between the growth phase and the stable phase when similar VEGF concentration was used. These results suggested that the released VEGF induced HUVEC proliferation and angiogenesis and the amount of VEGF produced during the growth phase and the stable phase were almost the same even though the production rate of VEGF was different between the growth phase and the stable phase.

We have confirmed that angiogenesis was strongly induced and the expressions of some tumor marker genes were suppressed during the stable phase. The essential features of tumor dormancy were described in the Introduction and our results match well with the described features. Therefore, we suggest that the stable phase of HepG2 cell culture in an RFB can be used as a tumor dormancy model, although some of genes were induced in the stable phase.

Effect of higher DO concentration during RFB cultivation Hermes *et al.* (29) showed that hypoxia showed the mRNA expression of the gene encoding erythropoietin and VEGF. VEGF expression was regulated by hypoxia-inducible factor-1(HIF-1) and the expression level of HIF-1 was increased in a hypoxic condition in HepG2 cell culture (30). To investigate the effects of DO on VEGF production rate in the RFB culture, we examined RFB cultivation at 8.0 ppm DO and measured VEGF concentration. VEGF productivity was lower than that at 4.0 ppm DO (Fig. 2), although it was still higher than those of the static culture and the growth phase. Below 8.0 ppm DO, the DO concentration of the inlet was approximately 16.0 ppm in the stable phase. This DO was 1.5-fold higher than that (10.0 ppm) below 4.0 ppm DO in the stable phase and we assumed that oxygen was sufficiently supplied to the cells in these two culture conditions in the RFB. Since there were no differences in glucose consumption rate, lactic acid production rate, glutamine consumption rate, and ammonia production rate between 4.0 ppm DO and 8.0 ppm DO, we considered that VEGF production was not affected under such high DO concentration. Moreover, HUVEC proliferation rate and blood vessel formation rate were almost the same (Fig. 3A, B). Platelet-derived growth factor (PDGF) and basic fibroblast growth factor (bFGF) are also known as angiogenesis inducing factors (31). We also measured the concentrations of PDGF and FGF in the conditioned medium of the RFB. However, PDGF and FGF were not detected (data not shown). Therefore, it was found that only the production of VEGF from HepG2 cells cultured in the RFB was strongly induced during the stable phase, whereas VEGF production induction was not regulated by DO concentration, and HUVEC proliferation rate and blood vessel formation rate were increased by the released VEGF. In the microarray analysis, the signal of HIF-1 was not induced in the stable phase compared with the growth phase and the static culture (data not shown). Mizukami *et al.* (32) showed that HIF-1 knock-down cells transplanted to mouse can induce angiogenesis and 50% the VEGF productivity of transplanted cells was maintained. This supported our results that the induction of VEGF during the stable phase of the RFB cultivation is not regulated by DO concentration. Therefore, RFB culture system may contribute to the construction of an *in vitro* model for angiogenesis or tumor progression and may provide an alternative method of tumor transplantation model to animals.

DISCUSSION

In our previous study, we demonstrated that the cultivation of HepG2 cells in a 5-ml RFB showed a high function similar to normal liver cells in the human body (8). To clarify cellular function in more detail, we performed DNA microarray analysis. The induced genes are listed in Table 1 and there was 18. Among the genes induced, we found that genes encoding some tumor marker proteins were induced during the stable growth phase rather than genes encoding liver specific functional proteins. In particular, the expressions of Grb10 and ATR1 have already been demonstrated in tumorigenic tissues (19, 20). Excluding these genes, six of the 18 induced genes were ones which were induced in tumor tissue. VEGF is a mitogen that specifically acts on endothelial cells and is a major regulator for the induction of angiogenesis in tumors (14, 15). Therefore, the cultivation of HepG2 cells in the RFB can be used as a three-dimensional growth model of tumors. However, the expression of some tumor suppressor genes have also been shown to be induced during the stable phase of the cell cycle (26, 27). In addition, we demonstrated in our previous study that most HepG2 cells during the stable phase remained in the G0/G1 phase (8). Therefore, we suggest that the RFB cultivation of HepG2 cells can be used as a model of tumor dormancy of highly proliferating tumors. Aguirre *et al.* (9) showed that the suppression of ERK signaling by the downregulation of urokinase plasminogen activator receptor induced tumor dormancy with G0/G1 arrest. As shown in Table 1, the induction of the expressions of IGFBP-3 and Grb10 has been demonstrated. IFGBP-3 has the ability to block the binding of IGF to the IGF receptor (33). Grb10 is known as a negative regulator of Grb2 which is a stimulator of the ERK signaling pathway (34). Thus, these proteins are associated with the suppression of IFG-receptor-mediated signal transduction pathway; the activation of this pathway stimulates cell proliferation via ERK activation (35). Our results from the microarray analysis suggest that cell cycle arrests during RFB cultivation in the stable phase may be induced by ERK inactivation via IGF receptor downregulation or a similar suppression of tyrosine kinase-receptor-mediated signal transduction pathway. Clinical experience in cancer patients showed that some primary cancers and most highly-metastatic cancer cells undergo dormancy before entering the stage of progressive growth (9). The cultivation of HepG2 cells in the RFB did not induce angiogenesis. Therefore, the RFB cultivation of cancer cells can be used as an *in vitro* model of tumor dormancy which is clinically observed in cancer patients.

In this report, we also show that the VEGF productivity of HepG2 cells cultivated in the RFB during the stable phase was threefold higher than that during the growth phase and static culture. The conditioned medium from the stable phase and the growth phase induced HUVEC proliferation and an-